WAVE PROPAGATION IN PIEZOELECTRIC MEDIUM WITH THE FLEXOELECTRIC EFFECT CONSIDERED

F. Y. Jiao **P. J. Wei***

Beijing Key Laboratory for Magneto-Photoelectrical Composite and Interface Science
University of Science and Technology Beijing
Beijing, China

Department of Applied Mechanics
University of Science and Technology Beijing
Beijing, China

Y. Q. Li

Department of Mathematics
Qiqihar University
Qiqihar, China

ABSTRACT

With the consideration of the flexoelectric effect, the dispersion feature of plane waves propagating in infinite piezoelectric medium and the reflection amplitude ratio at a mechanically traction-free and dielectrically charge-free surface of semi-infinite piezoelectric half-space are studied in this paper. The flexoelectric effect is essentially the microstructure effect of heterogeneous piezoelectric medium. Besides, the strain gradient effect and the micro-inertial effect are also introduced to reflect the influences of the microstructure. Different from the classical piezoelectric medium, there are five kinds of coupled elastic waves in the microstructured piezoelectric medium. The influences of the flexoelectric effect, the strain gradient effect and the micro-inertial effect upon the dispersion feature of the coupled elastic waves and the reflection amplitude ratio are studied numerically. The numerical results are shown graphically and are validated by the energy conservation law. It is found that these microstructure effects have obvious influences upon the dispersion feature of the coupled elastic waves and therefore also affect the reflection energy partition at the mechanically free surface. Especially, the micro-inertial effect has fundamental influences on the dispersion properties of the coupled elastic waves.

Keywords: Flexoelectric effect, Microstructure, Dispersion relation, Reflection.

1. INTRODUCTION

The wave propagation in piezoelectric medium has been studied extensively in the past decades. Alshits *et al*. [1, 2] studied various reflection problems of acoustic-electrically coupled waves in a semi-infinite piezoelectric medium with consideration of the metallized and non-metallized surfaces. Different from the purely elastic case, the acoustic waves propagating in piezoelectric solids are always accompanied by the waves of the quasi-static electric fields due to the electromechanical coupling effect. So these waves are also called acoustic-electrically coupled waves. Singh [3] studied the wave propagation in a prestressed piezoelectric half-space. The effect of initial stress on the reflection coefficients was discussed for a particular example of Lithium niobate. Pang *et al*. [4] studied the reflection and transmission of an elastic wave at the interface between the piezoelectric material ($BaTiO_3$) and the piezomagnetic material ($CoFeO_4$). It was found that there exist four independent basic waves in semi-infinite piezoelectric or piezomagnetic anisotropic elastic media. Abd-Alla and Alsheikh [5] studied the reflection and refraction of quasi-longitudinal waves under initial stresses at an interface of two anisotropic piezoelectric media with different properties. Guo and Wei [6, 7] studied not only the effects of initial stress but also the dielectrically imperfect interfaces on the reflection and transmission waves at the interface between two piezoelectric half spaces. Four kinds of dielectrically imperfect interfaces were considered in their work.

In the classical piezoelectric elastic theory, the stress at a material point is assumed to be dependent upon the strain and electric field at same material point, and no characteristic length is included in the constitutive relations. Therefore, the classical piezoelectric elastic theory cannot describe the mechanical and electrical behavior of piezoelectric material at the micro or nano scale

* Corresponding author (weipj@ustb.edu.cn)

DOI : 10.1017/jmech.2017.87
Copyright © 2017 The Society of Theoretical and Applied Mechanics
https://doi.org/10.1017/jmech.2017.87 Published online by Cambridge University Press

and the size effects. However, the situation is different until the find of the flexoelectric effect in nano-sized dielectrics. Zubko *et al*. [8] studied the flexoelectric effect in a piezoelectric solid. They discussed the presence of the flexoelectric effect in many nanoscale systems, and look at the potential applications of this electromechanical coupled phenomenon. Hu and Shen [9, 10] studied the variational principles and the governing equations in nano-dielectrics with the flexoelectric effect. By establishing the electric enthalpy variational principle for nano-sized dielectrics with the strain gradient and the polarization gradient effects, the governing equations and boundary conditions were given. Further, they also studied the electric field gradient theory with surface effects for nano-dielectrics. As regards the surface effects both the surface stress and surface polarization were considered. The governing equations and the generalized electromechanical Young-Laplace equations, which taken into account the effects of strain/electric field gradient, were derived. Shu *et al*. [11] studied the symmetry of flexoelectric coefficients in crystalline medium. It was indicated that the direct flexoelectric coefficients should be presented in 3 × 18 form and the converse flexoelectric coefficients in 6 × 9 form, rather than 6 × 6 form, like elastic constants. Qi *et al*. [12] studied size-dependent bending of an electro-elastic bilayer nano-beam due to the flexoelectricity and the strain gradient effect. The static bending problems of bilayer cantilever under closed and open circuit conditions were solved to show the size-dependency of the flexoelectric effect in both direct and converse flexoelectric processes. Numerical results demonstrated that both the strain gradient effect and the flexoelectric effect significantly influence the deflection of the bending cantilever when the beam thickness is comparable to the material length scale parameters. Liang *et al*. [13] studied Bernoulli–Euler dielectric beam model based on the strain-gradient theory. It was found that the deflection predicted by the strain gradient beam theory is smaller than that by the classical beam theory when the beam thickness is comparable to the internal length scale parameters and the external applied voltage obviously affect the deflection of the dielectric and piezoelectric nano-beam. Ebrahimi and Barati [14] investigated the vibration characteristics of a flexoelectric nanobeam in contact with Winkler-Pasternak foundation based on the nonlocal elasticity theory considering surface effects. Liu and Wang [15] investigated the size-dependent electromechanical properties of piezoelectric superlattices made of $BaTiO_3$ and $PbTiO_3$ layers, it was found that the strain gradient is giant at the interface between $BaTiO_3$ and $PbTiO_3$ layers, which will lead to the significant enhancement of polarization in the superlattice due to the flexoelectric effect, therefore, the influence of strain gradient at the interface becomes significant when the size of superlattice decreases. Although, the flexoelectric effect has been studied in the above-mentioned literatures, the investigation on the wave propagation in piezoelectric medium with the flexoelectric effect and the strain gradient effect taken into consideration has not been reported so far.

In this paper, the wave propagation in piezoelectric medium with the flexoelectric effect, the strain gradient effect and the micro-inertial effect taken into consideration is studied. The flexoelectric effect, the strain gradient effect and the micro-inertial effect are essentially the microstructure effects of heterogeneous piezoelectric medium. The flexoelectric effect reflects the micro electro-mechanically coupling. The strain gradient effect reflects the characteristic length of microstructure while the micro-inertial effect reflects the inertial characteristic length. The dispersion relations of various bulk waves in an infinite piezoelectric medium are derived and the influences of the flexoelectric effect and two characteristic lengths are studied numerically. Then the reflection problem at mechanically free surface is considered. The amplitude ratios and energy flux ratios of various reflection waves to the incident wave are calculated. The numerical results are validated by considering the energy conservation between the incident wave and reflection waves.

2. FORMULATION OF PROBLEM

The general expression of the electric Gibbs free energy density function can be written as [13]

$$U = -\frac{1}{2}\varepsilon_{kl}E_kE_l + \frac{1}{2}c_{ijkl}S_{ij}S_{kl} - e_{kij}E_kS_{ij} - f_{ijkl}E_i\eta_{jkl} + r_{ijklm}S_{ij}\eta_{klm} + \frac{1}{2}g_{ijklmn}\eta_{ijk}\eta_{lmn}, \tag{1}$$

where ε_{kl} and c_{ijkl} are the dielectric and the elastic tensors, respectively. e_{kij} is the piezoelectric tensor, f_{ijkl} is flexoelectric tensor, r_{ijklm} denotes the coupling between the strain and strain gradient. The tensor g_{ijklmn} represents the strain gradient effect. S_{ij} is the strain tensor, η_{ijk} is the strain gradient tensor and E_i is the electric field vector, which are defined, respectively, as $S_{ij} = (u_{j,i} + u_{i,j})/2$, $\eta_{ijk} = S_{ij,k}$ and $E_i = -\varphi_{,i}$, where u_i is the displacement, $\varphi$is the electric potential, the comma indicates differentiation with respect to the spatial variables.

It is noted that

$$\int_V r_{ijklm}S_{ij}\eta_{klm}dV = \frac{1}{2}\int_V r_{ijklm}\left(S_{ij}S_{kl}\right)_{,m}dV = \frac{1}{2}\int_S \left(S_{ij}S_{kl}\right)r_{ijklm}n_m dS, \quad (r_{ijklm}=r_{klijm}) \tag{2}$$

This means that the fifth term in the right hand side of the Eq. (1) is the contribution from the surface of material. Let

$$U^s = \frac{1}{2}r_{ijklm}S_{ij}\eta_{klm} \tag{3}$$

Then, U^s is the surface energy of unit surface area and it incorporates the contribution from the surface stresses. In the present work, the surface effects of material are neglected, namely, r_{ijklm} is null. Moreover, g_{jkhmni} is approximated by [16] $g_{jkhmni} = l_1^2\delta_{hi}c_{jkmn}$, where l_1 is in-

https://doi.org/10.1017/jmech.2017.87 Published online by Cambridge University Press

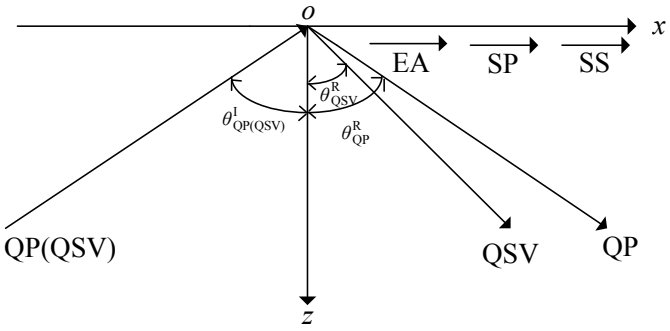


Fig. 1 Reflection waves at the mechanically free surface for an incident quasi-longitudinal wave (QP) or quasi-traverse wave (QSV).

ternal characteristic length of microstructure. Then, the constitutive equations can be obtained from the electric Gibbs free energy as

$$\sigma_{ij} = c_{ijkl} S_{kl} - e_{kij} E_k, \tag{4a}$$

$$\sigma_{jkh} = -f_{ijkh} E_i + l_1^2 \delta_{hi} c_{jkmn} \eta_{mni}, \tag{4b}$$

$$D_k^e = \varepsilon_{kl} E_l + e_{kij} S_{ij} + f_{klmn} \eta_{lmn}, \tag{4c}$$

where, σ_{ij} is the classical Cauchy stress tensor, σ_{jkh} is the higher-order stress tensor, and D_k^e is the electric displacement vector. It is noted that $\sigma_{ij} = \sigma_{ji}$ and $\sigma_{jkh} = \sigma_{kjh}$.

Let the z-axis be the poling direction and the material is assumed to be transversely isotropic in the oxy coordinate plane, see Fig. 1. Then, the Eqs. (4a, 4b, 4c) reduce to [11]

$$\begin{Bmatrix} \sigma_{xx} \\ \sigma_{yy} \\ \sigma_{zz} \\ \sigma_{yz} \\ \sigma_{zx} \\ \sigma_{xy} \end{Bmatrix} = \begin{bmatrix} c_{11} & c_{12} & c_{13} & 0 & 0 & 0 \\ c_{12} & c_{11} & c_{13} & 0 & 0 & 0 \\ c_{13} & c_{13} & c_{33} & 0 & 0 & 0 \\ 0 & 0 & 0 & c_{44} & 0 & 0 \\ 0 & 0 & 0 & 0 & c_{44} & 0 \\ 0 & 0 & 0 & 0 & 0 & 0.5(c_{11} - c_{12}) \end{bmatrix} \cdot \begin{Bmatrix} S_{xx} \\ S_{yy} \\ S_{zz} \\ 2S_{yz} \\ 2S_{zx} \\ 2S_{xy} \end{Bmatrix} - \begin{bmatrix} 0 & 0 & e_{31} \\ 0 & 0 & e_{31} \\ 0 & 0 & e_{33} \\ 0 & e_{15} & 0 \\ e_{15} & 0 & 0 \\ 0 & 0 & 0 \end{bmatrix} \cdot \begin{Bmatrix} E_x \\ E_y \\ E_z \end{Bmatrix}, \tag{5a}$$

$$\begin{Bmatrix} \boldsymbol{\sigma}_{xx} \\ \boldsymbol{\sigma}_{yy} \\ \boldsymbol{\sigma}_{zz} \\ \boldsymbol{\sigma}_{yz} \\ \boldsymbol{\sigma}_{zx} \\ \boldsymbol{\sigma}_{xy} \end{Bmatrix} = -\begin{bmatrix} \mathbf{M}_1 \\ \mathbf{M}_2 \\ \mathbf{M}_3 \\ \mathbf{M}_4 \\ \mathbf{M}_5 \\ \mathbf{M}_6 \end{bmatrix} \cdot \begin{Bmatrix} E_x \\ E_y \\ E_z \end{Bmatrix} + \mathbf{G} \cdot \begin{Bmatrix} \boldsymbol{\eta}_{xx} \\ \boldsymbol{\eta}_{yy} \\ \boldsymbol{\eta}_{zz} \\ 2\boldsymbol{\eta}_{yz} \\ 2\boldsymbol{\eta}_{zx} \\ 2\boldsymbol{\eta}_{xy} \end{Bmatrix}, \tag{5b}$$

$$\begin{Bmatrix} D_x^e \\ D_y^e \\ D_z^e \end{Bmatrix} = \begin{bmatrix} 0 & 0 & 0 & 0 & e_{15} & 0 \\ 0 & 0 & 0 & e_{15} & 0 & 0 \\ e_{31} & e_{31} & e_{33} & 0 & 0 & 0 \end{bmatrix} \cdot \begin{Bmatrix} S_{xx} \\ S_{yy} \\ S_{zz} \\ 2S_{yz} \\ 2S_{zx} \\ 2S_{xy} \end{Bmatrix} + \begin{bmatrix} \varepsilon_{11} & 0 & 0 \\ 0 & \varepsilon_{11} & 0 \\ 0 & 0 & \varepsilon_{33} \end{bmatrix} \cdot \begin{Bmatrix} E_x \\ E_y \\ E_z \end{Bmatrix}$$

$$+ \begin{bmatrix} \mathbf{M}_1 & \mathbf{M}_2 & \mathbf{M}_3 & \mathbf{M}_4 & \mathbf{M}_5 & \mathbf{M}_6 \end{bmatrix} \cdot \begin{Bmatrix} \boldsymbol{\eta}_{xx} \\ \boldsymbol{\eta}_{yy} \\ \boldsymbol{\eta}_{zz} \\ 2\boldsymbol{\eta}_{yz} \\ 2\boldsymbol{\eta}_{zx} \\ 2\boldsymbol{\eta}_{xy} \end{Bmatrix}, \tag{5c}$$

https://doi.org/10.1017/jmech.2017.87 Published online by Cambridge University Press

where

$$\boldsymbol{\sigma}_{xx}=\begin{Bmatrix}\sigma_{xxx}\\ \sigma_{xxy}\\ \sigma_{xxz}\end{Bmatrix},\quad \boldsymbol{\sigma}_{yy}=\begin{Bmatrix}\sigma_{yyx}\\ \sigma_{yyy}\\ \sigma_{yyz}\end{Bmatrix},\quad \boldsymbol{\sigma}_{zz}=\begin{Bmatrix}\sigma_{zzx}\\ \sigma_{zzy}\\ \sigma_{zzz}\end{Bmatrix},\quad \boldsymbol{\sigma}_{yz}=\begin{Bmatrix}\sigma_{yzx}\\ \sigma_{yzy}\\ \sigma_{yzz}\end{Bmatrix},\quad \boldsymbol{\sigma}_{zx}=\begin{Bmatrix}\sigma_{zxx}\\ \sigma_{zxy}\\ \sigma_{zxz}\end{Bmatrix},\quad \boldsymbol{\sigma}_{xy}=\begin{Bmatrix}\sigma_{xyx}\\ \sigma_{xyy}\\ \sigma_{xyz}\end{Bmatrix}.$$

$$\mathbf{M}_1=\begin{bmatrix}\mu_{11}&0&0\\0&\mu_{14}&0\\0&0&\mu_{14}\end{bmatrix},\quad \mathbf{M}_2=\begin{bmatrix}\mu_{14}&0&0\\0&\mu_{11}&0\\0&0&\mu_{14}\end{bmatrix},\quad \mathbf{M}_3=\begin{bmatrix}\mu_{14}&0&0\\0&\mu_{14}&0\\0&0&\mu_{11}\end{bmatrix},\quad \mathbf{M}_4=\begin{bmatrix}0&0&0\\0&0&\mu_{111}\\0&\mu_{111}&0\end{bmatrix},$$

$$\mathbf{M}_5=\begin{bmatrix}0&0&\mu_{111}\\0&0&0\\\mu_{111}&0&0\end{bmatrix},\quad \mathbf{M}_6=\begin{bmatrix}0&\mu_{111}&0\\\mu_{111}&0&0\\0&0&0\end{bmatrix}.$$

$$\boldsymbol{\eta}_{xx}=\begin{Bmatrix}\eta_{xxx}\\ \eta_{xxy}\\ \eta_{xxz}\end{Bmatrix},\quad \boldsymbol{\eta}_{yy}=\begin{Bmatrix}\eta_{yyx}\\ \eta_{yyy}\\ \eta_{yyz}\end{Bmatrix},\quad \boldsymbol{\eta}_{zz}=\begin{Bmatrix}\eta_{zzx}\\ \eta_{zzy}\\ \eta_{zzz}\end{Bmatrix},\quad \boldsymbol{\eta}_{yz}=\begin{Bmatrix}\eta_{yzx}\\ \eta_{yzy}\\ \eta_{yzz}\end{Bmatrix},\quad \boldsymbol{\eta}_{zx}=\begin{Bmatrix}\eta_{zxx}\\ \eta_{zxy}\\ \eta_{zxz}\end{Bmatrix},\quad \boldsymbol{\eta}_{xy}=\begin{Bmatrix}\eta_{xyx}\\ \eta_{xyy}\\ \eta_{xyz}\end{Bmatrix}.$$

$$\mathbf{G}=l_1^2\begin{bmatrix}\mathbf{G}_{11}&\mathbf{G}_{12}&\mathbf{G}_{13}\\ \mathbf{G}_{21}&\mathbf{G}_{22}&\mathbf{G}_{23}\\ \mathbf{G}_{31}&\mathbf{G}_{32}&\mathbf{G}_{33}\end{bmatrix}.$$

The explicit expressions of elements in the matrix **G** are given in Appendix A.
In the plane strain case, the displacement and the electric potential are the function of only x and z, namely,

$$\boldsymbol{u}=\{u(x,z,t),0,w(x,z,t)\},\quad \varphi=\varphi(x,z,t). \tag{6a,b}$$

By using the displacements and the electric potential as the basic qualities, we obtain

$$\sigma_{xx}=c_{11}\frac{\partial u}{\partial x}+c_{13}\frac{\partial w}{\partial z}+e_{31}\frac{\partial \varphi}{\partial z},\quad \sigma_{yy}=c_{12}\frac{\partial u}{\partial x}+c_{13}\frac{\partial w}{\partial z}+e_{31}\frac{\partial \varphi}{\partial z}, \tag{7a,b}$$

$$\sigma_{zz}=c_{13}\frac{\partial u}{\partial x}+c_{33}\frac{\partial w}{\partial z}+e_{33}\frac{\partial \varphi}{\partial z},\quad \sigma_{zx}=c_{44}\left(\frac{\partial u}{\partial z}+\frac{\partial w}{\partial x}\right)+e_{15}\frac{\partial \varphi}{\partial x},\quad \sigma_{yz}=\sigma_{xy}=0. \tag{7c,d,e}$$

$$\sigma_{xxx}=\mu_{11}\frac{\partial \varphi}{\partial x}+l_1^2c_{11}\frac{\partial^2 u}{\partial x^2}+l_1^2c_{13}\frac{\partial^2 w}{\partial x\partial z},\quad \sigma_{xxz}=\mu_{14}\frac{\partial \varphi}{\partial z}+l_1^2c_{11}\frac{\partial^2 u}{\partial x\partial z}+l_1^2c_{13}\frac{\partial^2 w}{\partial z^2}, \tag{8a,b}$$

$$\sigma_{yyx}=\mu_{14}\frac{\partial \varphi}{\partial x}+l_1^2c_{12}\frac{\partial^2 u}{\partial x^2}+l_1^2c_{13}\frac{\partial^2 w}{\partial x\partial z},\quad \sigma_{yyz}=\mu_{14}\frac{\partial \varphi}{\partial z}+l_1^2c_{12}\frac{\partial^2 u}{\partial x\partial z}+l_1^2c_{13}\frac{\partial^2 w}{\partial z^2}, \tag{8c,d}$$

$$\sigma_{zzx}=\mu_{14}\frac{\partial \varphi}{\partial x}+l_1^2c_{13}\frac{\partial^2 u}{\partial x^2}+l_1^2c_{33}\frac{\partial^2 w}{\partial x\partial z},\quad \sigma_{zzz}=\mu_{11}\frac{\partial \varphi}{\partial z}+l_1^2c_{13}\frac{\partial^2 u}{\partial x\partial z}+l_1^2c_{33}\frac{\partial^2 w}{\partial z^2}, \tag{8e,f}$$

$$\sigma_{yzy}=\sigma_{zyy}=\mu_{111}\frac{\partial \varphi}{\partial z},\quad \sigma_{zxx}=\sigma_{xzx}=\mu_{111}\frac{\partial \varphi}{\partial z}+l_1^2c_{44}\left(\frac{\partial^2 u}{\partial x\partial z}+\frac{\partial^2 w}{\partial x^2}\right), \tag{8g,h}$$

$$\sigma_{zxz}=\sigma_{xzz}=\mu_{111}\frac{\partial \varphi}{\partial x}+l_1^2c_{44}\left(\frac{\partial^2 w}{\partial x\partial z}+\frac{\partial^2 u}{\partial z^2}\right),\quad \sigma_{xyy}=\sigma_{yxy}=\mu_{111}\frac{\partial \varphi}{\partial x}, \tag{8i,j}$$

$$\sigma_{xxy}=\sigma_{yyy}=\sigma_{zzy}=\sigma_{zxy}=\sigma_{xzy}=\sigma_{yzx}=\sigma_{zyx}=\sigma_{yzz}=\sigma_{zyz}=\sigma_{xyx}=\sigma_{yxx}=\sigma_{xyz}=\sigma_{yxz}=0. \tag{8k}$$

$$D_x^e=e_{15}\left(\frac{\partial u}{\partial z}+\frac{\partial w}{\partial x}\right)-\varepsilon_{11}\frac{\partial \varphi}{\partial x}+\mu_{11}\frac{\partial^2 u}{\partial x^2}+\mu_{14}\frac{\partial^2 w}{\partial x\partial z}+\mu_{111}\left(\frac{\partial^2 u}{\partial z^2}+\frac{\partial^2 w}{\partial x\partial z}\right), \tag{9a}$$

$$D_y^e=0, \tag{9b}$$

https://doi.org/10.1017/jmech.2017.87 Published online by Cambridge University Press

$$D_z^e = e_{31}\frac{\partial u}{\partial x} + e_{33}\frac{\partial w}{\partial z} - \varepsilon_{33}\frac{\partial \varphi}{\partial z} + \mu_{11}\frac{\partial^2 w}{\partial z^2} + \mu_{14}\frac{\partial^2 u}{\partial x \partial z} + \mu_{111}\left(\frac{\partial^2 w}{\partial x^2} + \frac{\partial^2 u}{\partial x \partial z}\right). \tag{9c}$$

The kinetic energy density with consideration of the micro-inertial effect can be expressed as [17]

$$T = \frac{1}{2}\rho \dot{u}_j \dot{u}_j + \frac{1}{6}\rho l_2^2 \dot{u}_{k,j}\dot{u}_{k,j}, \tag{10}$$

where ρ is mass density, and l_2 is the micro inertia characteristic length which reflects the micro-inertial effect. Then, the variation of the electric Gibbs free energy density (electrostatic force is neglected) plus the kinetic energy density are [9, 10, 17]

$$\begin{aligned}\delta\int_V (U+T)dV = &\int_a \left[\left(\sigma_{ij} - \sigma_{ijm,m}\right)n_j + D_l\left(n_l\right)\sigma_{ijm}n_j n_m - D_j\left(\sigma_{ijm}n_m\right) + \frac{\rho l_2^2}{3}n_j\ddot{u}_{i,j}\right]\delta u_i da - \int_V D^e_{m,m}\delta\varphi dV \\ &- \int_V \left[\left(\sigma_{ij} - \sigma_{ijm,m}\right)_{,j} - \left(\rho\ddot{u}_i - \frac{\rho l_2^2}{3}\ddot{u}_{i,jj}\right)\right]\delta u_i dV + \int_a \sigma_{ijm}n_j n_m D\delta u_i da + \int_a n_i D_i^e \delta\varphi da,\end{aligned} \tag{11}$$

where n_j is the unit normal vector of the boundary of solid, $D_j(\ ) = (\ )_{,j} - n_j n_k (\ )_{,k}$, $D(\ ) = n_l(\ )_{,l}$.

The variation of work done by external forces can be expressed as

$$\delta W = \int_V F_i \delta u_i dV + \int_a P_i \delta u_i da + \int_a R_i D\delta u_i da + \int_a q\delta\varphi da, \tag{12}$$

where F_i is the body force (it is neglected in following), P_i is the monopolar traction, R_i is the dipolar traction and q is the charge. According to the variation principle

$$\delta\int_V (U+T)dV = \delta W, \tag{13}$$

the mechanical and electric governing equations, and the monopolar and dipolar tractions can be expressed as

$$\left(\sigma_{ij} - \sigma_{ijm,m}\right)_{,j} = \rho\ddot{u}_i - \frac{\rho l_2^2}{3}\ddot{u}_{i,jj}, \quad D^e_{m,m} = 0. \tag{14a,b}$$

$$P_i = \left(\sigma_{ij} - \sigma_{ijm,m}\right)n_j + D_l\left(n_l\right)\sigma_{ijm}n_j n_m - D_j\left(\sigma_{ijm}n_m\right) + \frac{\rho l_2^2}{3}n_j\ddot{u}_{i,j}, \tag{15a}$$

$$R_i = \sigma_{ijm}n_j n_m, \quad q = n_i D_i^e. \tag{15b,c}$$

For the wave propagation problem, the solution of Eq. (14) is of the form

$$\{u, w, \varphi\} = \{U_1, U_2, U_3\}\exp\left[\mathrm{i}\xi\left(x + \alpha z - ct\right)\right], \tag{16}$$

where $\xi(=k_x = k\sin\theta)$ and c are the apparent wavenumber and the apparent speed, respectively. $\alpha = k_z/k_x$ is the projection ratio of wave number. Inserting Eq. (16) into Eq. (14) leads to

$$\begin{bmatrix} K_{11} & K_{12} & K_{13} \\ K_{21} & K_{22} & K_{23} \\ K_{31} & K_{32} & K_{33} \end{bmatrix} \cdot \begin{Bmatrix} U_1 \\ U_2 \\ U_3 \end{Bmatrix} = \begin{Bmatrix} 0 \\ 0 \\ 0 \end{Bmatrix}. \tag{17}$$

The explicit expressions of elements in the matrix **K** are given in Appendix B. The condition of existing non-trivial solution is

$$\left|K_{ij}(c, \alpha, \omega)\right|_{3\times 3} = 0. \tag{18}$$

It is the dispersive equation of wave propagation. In general, for a given apparent wave speed c and angular frequency ω, Eq. (18) is a polynomial of ten orders about α. The solutions of this polynomial stand for all possible wave modes. The real value of α stands for the bulk wave propagates in the oxz plane. The imaginary value of α stands for the surface wave propagates along the boundary. The complex value of α stands for the bulk wave with decreasing or

https://doi.org/10.1017/jmech.2017.87 Published online by Cambridge University Press

increasing amplitude accompanied with propagation. This type of wave is physically unacceptable in the elastic solid without dissipation. For the transversely isotropic half-space considered, the value of α indicates that there are ten possible partial waves. Four of them are bulk waves and six of them are the surface waves. Moreover, two bulk waves are of the wave vector with positive projection along z axis while the other two bulk waves are of wave vector with negative projection along z axis. Therefore, the four bulk waves are the incident and reflection waves, respectively. Let α_1, α_3, α_5, α_7 and α_9 are the reflection quasi-longitudinal wave (QP), the reflection quasi-traverse wave (QSV), the reflection electric–acoustic wave (EA), the reflection P-type surface wave (SP) and reflection S-type surface wave (SS); while α_2, α_4, α_6, α_8 and α_{10} are the incident QP wave, incident QSV wave, incident EA wave, incident SP wave and incident SS wave. The incident and reflection angle θ_q can be determined by $\cos\theta_q = \text{Real}(\alpha_q)$.

Define the amplitude ratios of each coupled wave (q = 1, 2, …, 10)

$$G_q = \frac{U_{2q}}{U_{1q}} = \frac{K_{21}(\alpha_q)\cdot K_{13}(\alpha_q) - K_{11}(\alpha_q)\cdot K_{23}(\alpha_q)}{K_{12}(\alpha_q)\cdot K_{23}(\alpha_q) - K_{13}(\alpha_q)\cdot K_{22}(\alpha_q)}. \tag{19a}$$

$$H_q = \frac{U_{3q}}{U_{1q}} = \frac{K_{11}(\alpha_q)\cdot K_{22}(\alpha_q) - K_{12}(\alpha_q)\cdot K_{21}(\alpha_q)}{K_{12}(\alpha_q)\cdot K_{23}(\alpha_q) - K_{13}(\alpha_q)\cdot K_{22}(\alpha_q)}. \tag{19b}$$

Then, the displacement, the electric potential, the classical Cauchy stress, the electric displacement and the higher-order stress created by the incident wave and reflection waves can be expressed as

$$\{u, w, \varphi\} = \sum_{q=1}^{10} \{1, G_q, H_q\} U_{1q} \exp\left[\mathrm{i}\xi\left(x + \alpha_q z - ct\right)\right], \tag{20}$$

$$\{\sigma_{zx}, \sigma_{zz}, \sigma_{xx}\} = \sum_{q=1}^{10} \mathrm{i}\xi \{F_{1q}, F_{2q}, F_{3q}\} U_{1q} \exp\left[\mathrm{i}\xi\left(x + \alpha_q z - ct\right)\right], \tag{21}$$

$$\left\{D_z^e, D_x^e\right\} = \sum_{q=1}^{10} \mathrm{i}\xi \{F_{4q}, F_{5q}\} U_{1q} \exp\left[\mathrm{i}\xi\left(x + \alpha_q z - ct\right)\right], \tag{22}$$

$$\{\sigma_{zxx}, \sigma_{zxz}, \sigma_{zzx}, \sigma_{zzz}, \sigma_{xxx}, \sigma_{xxz}\} = \sum_{q=1}^{10} \{F_{6q}, F_{7q}, F_{8q}, F_{9q}, F_{10q}, F_{11q}\} U_{1q} \exp\left[\mathrm{i}\xi\left(x + \alpha_q z - ct\right)\right]. \tag{23}$$

The explicit expressions of F_{iq} (i = 1 − 11) are given in Appendix C, and $\{1, G_q, H_q\}$ is the vibration form vector of each coupled wave.

At the boundary, i.e. $\mathbf{n} = \mathbf{e}_z$, the monopolar, the dipolar tractions and the charge density can be expressed as

$$P_i = \sigma_{iz} - \sigma_{izx,x} - \sigma_{izz,z} - \sigma_{ixz,x} + \rho l_2^2 \ddot{u}_{i,z} / 3 \quad (i = x, z), \tag{24a}$$

$$R_i = \sigma_{izz} \ (i = x, z), \quad q = D_z^e. \tag{24b,c}$$

Inserting Eqs. (20)-(23) into (24) leads to

$$P_x = \sum_{q=1}^{10} \mathrm{i}\xi M_{1q} U_{1q} \exp\left[\mathrm{i}\xi\left(x + \alpha_q z - ct\right)\right], \tag{25a}$$

$$P_z = \sum_{q=1}^{10} \mathrm{i}\xi M_{2q} U_{1q} \exp\left[\mathrm{i}\xi\left(x + \alpha_q z - ct\right)\right], \tag{25b}$$

$$R_x = \sum_{q=1}^{10} M_{3q} U_{1q} \exp\left[\mathrm{i}\xi\left(x + \alpha_q z - ct\right)\right], \tag{25c}$$

$$R_z = \sum_{q=1}^{10} M_{4q} U_{1q} \exp\left[\mathrm{i}\xi\left(x + \alpha_q z - ct\right)\right], \tag{25d}$$

$$q = \sum_{q=1}^{10} \mathrm{i}\xi M_{5q} U_{1q} \exp\left[\mathrm{i}\xi\left(x + \alpha_q z - ct\right)\right], \tag{25e}$$

https://doi.org/10.1017/jmech.2017.87 Published online by Cambridge University Press

Table 1 The physical constants of $BaTiO_3$ [4].

	C_{11}	C_{33}	C_{13}	C_{44}	e_{31}	e_{33}	e_{15}	ε_{11}	ε_{33}	ρ
$BaTiO_3$	166	162	78	43	-4.4	18.6	11.6	11.2	12.6	5800

C_{ij}: (GPa), e_{ij}: (C/m^2), ε_{ij}: ($10^{-9}C^2/Nm^2$), ρ: (Kg/m^3).

where

$$M_{1q} = F_{1q} - F_{6q} - F_{7q}\alpha_q - F_{11q} - \rho l_2^2 \xi^2 c^2 \alpha_q / 3,$$

$$M_{2q} = F_{2q} - F_{8q} - F_{9q}\alpha_q - F_{7q} - \rho l_2^2 \xi^2 c^2 G_q \alpha_q / 3,$$

$$M_{3q} = F_{7q}, \quad M_{4q} = F_{9q}, \quad M_{5q} = F_{4q}.$$

The boundary condition, namely, mechanically traction-free and dielectrically charge-free,

$$P_x = 0, \quad P_z = 0, \quad R_x = 0, \quad R_z = 0, \quad q = 0 \quad \text{at} \quad z = 0. \tag{26}$$

leads to

$$\begin{bmatrix} M_{11} & M_{13} & M_{15} & M_{17} & M_{19} \\ M_{21} & M_{23} & M_{25} & M_{27} & M_{29} \\ M_{31} & M_{33} & M_{35} & M_{37} & M_{39} \\ M_{41} & M_{43} & M_{45} & M_{47} & M_{49} \\ M_{51} & M_{53} & M_{55} & M_{57} & M_{59} \end{bmatrix} \cdot \begin{Bmatrix} L_1 \\ L_2 \\ L_3 \\ L_4 \\ L_5 \end{Bmatrix} = - \begin{Bmatrix} M_{1q} \\ M_{2q} \\ M_{3q} \\ M_{4q} \\ M_{5q} \end{Bmatrix}, \tag{27}$$

where $L_1 = U_{11}/U_{1q}$, $L_2 = U_{13}/U_{1q}$, $L_3 = U_{15}/U_{1q}$, $L_4 = U_{17}/U_{1q}$, $L_5 = U_{19}/U_{1q}$ are the amplitude ratios of various reflection waves. q = 2 indicates the incident QP wave and q = 4 indicates the incident QSV wave, see Fig. 1.

Now, let us examine the energy fluxes conservation between the incident wave and reflection waves. The normal energy fluxes carried by the bulk waves are

$$Q(t) = -P_i \dot{u}_i - R_i n_j \dot{u}_{i,j} + \varphi n_i \dot{D}_i^e, \tag{28}$$

where the first term in the right hand side is related to the work rate done by the monopolar tractions, the second term to the work rate done by the dipolar tractions and the third term to the work rate done by the electric field. The average normal energy fluxes of the bulk waves in a period can be defined as

$$\bar{Q} = \frac{1}{T}\int_0^T Q(t)dt. \tag{29}$$

Inserting Eqs. (20) and (25) into Eqs. (28) and (29) leads to

$$\bar{Q} = \frac{1}{2}\xi^2 c\left(M_{1q} + M_{2q}G_q^* - M_{3q}\alpha_q^* - M_{4q}G_q^*\alpha_q^* + H_q M_{5q}^*\right) \times\left(U_{1q}\cdot U_{1q}^*\right), \tag{30}$$

where superscript "*" indicates the conjugated complex. Define the ratios of the average energy fluxes of the reflection waves to the incident wave as the energy reflection coefficients, i.e.

$$E_{QP}^R = \frac{\bar{Q}_{QP}^R}{\bar{Q}_{QP(QSV)}^I}, \quad E_{QSV}^R = \frac{\bar{Q}_{QSV}^R}{\bar{Q}_{QP(QSV)}^I}. \tag{31}$$

The energy flux conservation requires

$$E_{QP}^R + E_{QSV}^R = 1. \tag{32}$$

3. NUMERICAL RESULTS AND DISCUSSION

It is known that the dispersion curves and reflection coefficients L_i (i = 1 – 5) are both dependent upon the material constants of piezoelectric solid, the angular frequency ω and incident angle θ of the incident wave. In the present numerical example, the main concerns focus on the influences of the flexoelectric coefficients and two characteristic lengths of microstructure. For convenience, the following non-dimensional forms of material parameters are introduced, namely, $\bar{l}_1 = l_1/\lambda$, $\bar{l}_2 = l_2/\lambda$, $\bar{\mu}_{11} = \mu_{11}/\lambda e_{33}$, $\bar{\mu}_{14} = \mu_{14}/\lambda e_{33}$, $\bar{\mu}_{111} = \mu_{111}/\lambda e_{33}$, where λ is the wave length of incident wave. The reflection waves at the free surface of the piezoelectric solid $BaTiO_3$ are considered and the material constants of $BaTiO_3$ are listed in Table 1.

Figure 2 shows the influences of the flexoelectric coefficients and two characteristic lengths of microstructure on the dispersion curves of the QP wave which propagates with the angle θ = 30° from z axis. $\bar{c}_{QP}$ in Fig. 2 is the ratio of wave speed that QP wave propagates in flexoelectric piezoelectric medium and classical piezoelectric medium with the same propagation direction. It is observed that the flexoelectric effect make the propagation velocity of QP wave increase evidently, see Fig. 2(a). The static characteristic length of microstructure, l_1 has similar influences with the flexoelectric coefficients, see Fig. 2(c). However, the inertial characteristic length of microstructure, l_2 has completely different influences, see Fig. 2(d). When the inertial characteristic length l_2 is equal to zero, the propagation velocity c_{QP} will tend to infinite as the frequency increases gradually, see Fig. 2(b). This is unacceptable physically. When the inertial characteristic length l_2 is not equal to zero, the propagation velocity c_{QP} will tend asymptotically to a finite value as the frequency increases gradually, see Fig. 2(a) and Fig. 2(c). This means that the inertial characteristic length l_2 is a vital parameter in order to exhibit a correct dispersive feature at the high frequency range.

https://doi.org/10.1017/jmech.2017.87 Published online by Cambridge University Press

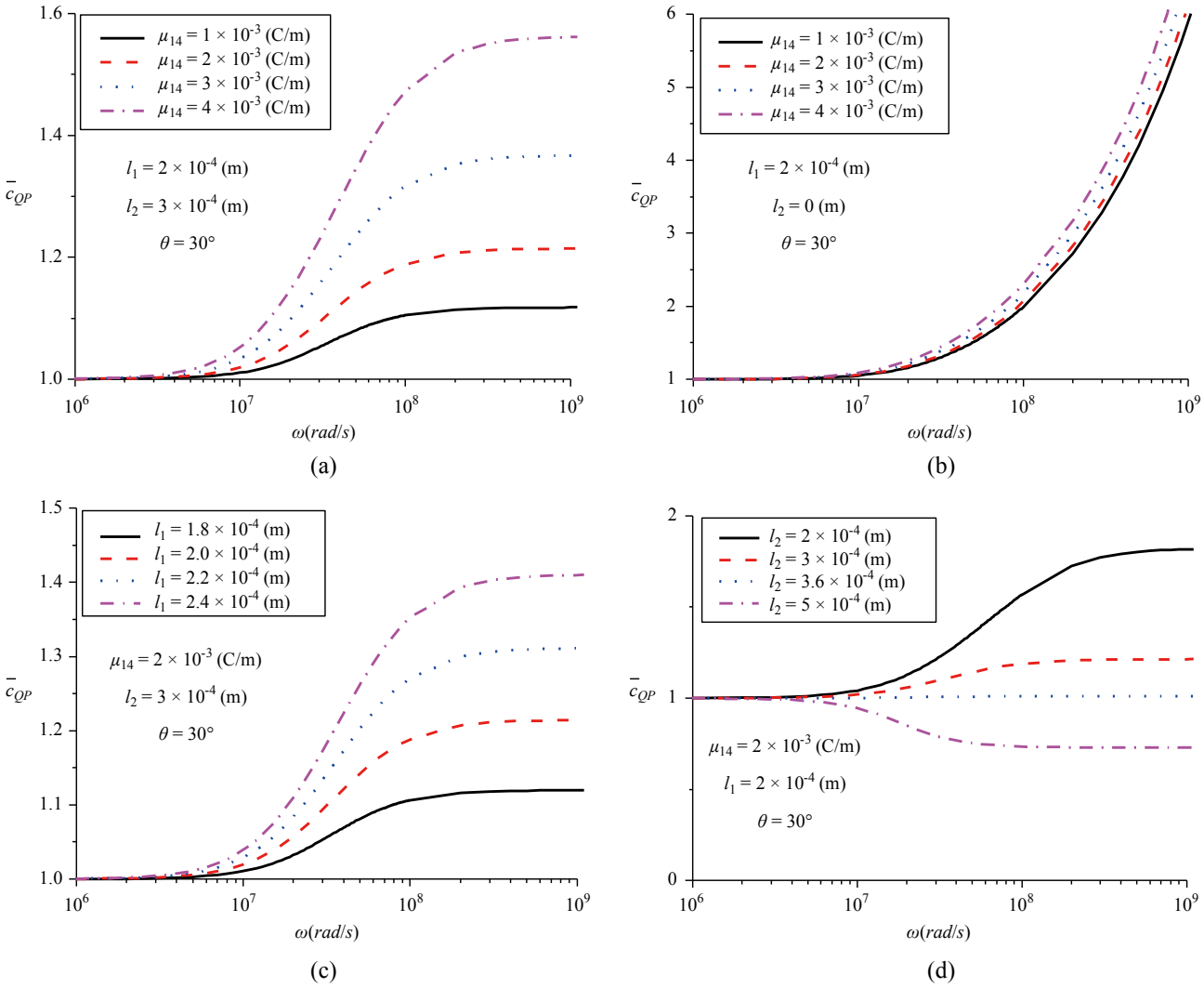


Fig.2 The influences of flexoelectric coefficients and two characteristic lengths on the dispersion curves of the QP wave. ($\mu_{11} = 0.5\mu_{14}, \mu_{111} = 2\mu_{14}$)

Furthermore, it is also observed that the phase speeds of QP waves will be greater, equal and smaller than that in the classic elastic solids (without the microstructure effects considered) as the inertial characteristic length l_2 takes different values, see Fig. 2(d). Even, at certain value, the dispersive feature disappears, namely, the dispersive QP wave becomes nondispersive.

Figure 3 shows the influences of the flexoelectric effect on the amplitude ratios of various reflection waves in the case of incident QP wave. It is observed that the influences of the flexoelectric effect are much greater upon the surface waves (EA wave, SP wave and SS wave) than bulk waves (QP wave and QSV wave). The similar phenomenon is also observed for the two characteristic lengths, namely, the influences of two characteristic lengths are mainly concentrated on the reflection surface waves. This phenomenon can be explained by that the reflection surface waves, SP wave and SS wave, are created due to the microstructure effects and therefore are sensitive to the microstructure parameters. Figure 4 shows the influences of the flexoelectric effect in the case of incident QSV wave. Similar phenomenon is observed, namely, the various reflection surface waves are more sensitive to the flexoelectric effect than the reflection bulk waves. Moreover, it is noticed that the influences of the flexoelectric effect are more evident in the incident QSV wave situation compared with the incident QP wave. In the situation of incident QSV wave, there is a critical angle (about 31.7^0) corresponding with that the reflection QP wave becomes the surface wave. At the vicinity of the critical angle, the reflection coefficients change dramatically, in general. The reflection coefficients tend to zero when the incident wave is close to the grazing incidence. For the purpose of comparison, the amplitude ratios for the classical piezoelectric solid (without consideration of the microstructure effects) are also provided in Fig. 3 and Fig. 4. The deviations between the piezoelectric solids with and without the microstructure effects actually result from the flexoelectric effect, the strain gradient effect and the micro-inertial effect. The present work emphasized particularly on the flexoelectric effect. In order to validate the numerical results, the energy conservation between the incident wave and the reflection waves are also

https://doi.org/10.1017/jmech.2017.87 Published online by Cambridge University Press

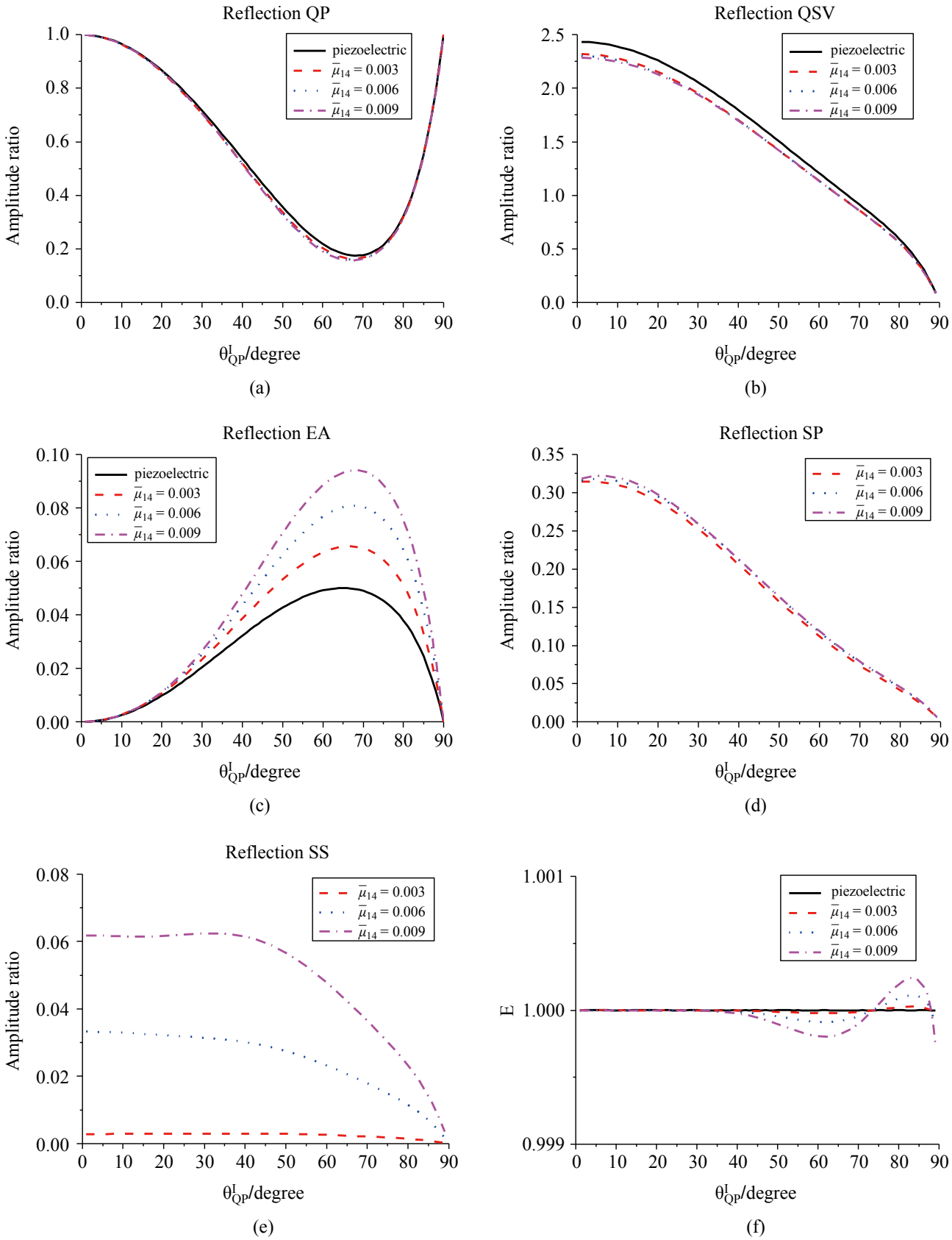


Fig. 3 The influences of flexoelectric coefficients on the amplitude ratios in the case of incident QP wave and the check on the energy flux conservation. ($\bar{\mu}_{11} = 0.5\bar{\mu}_{14}$, $\bar{\mu}_{111} = 2\bar{\mu}_{14}$, $\bar{l}_1$=0.03 , $\bar{l}_2 = 0.03$).

https://doi.org/10.1017/jmech.2017.87 Published online by Cambridge University Press

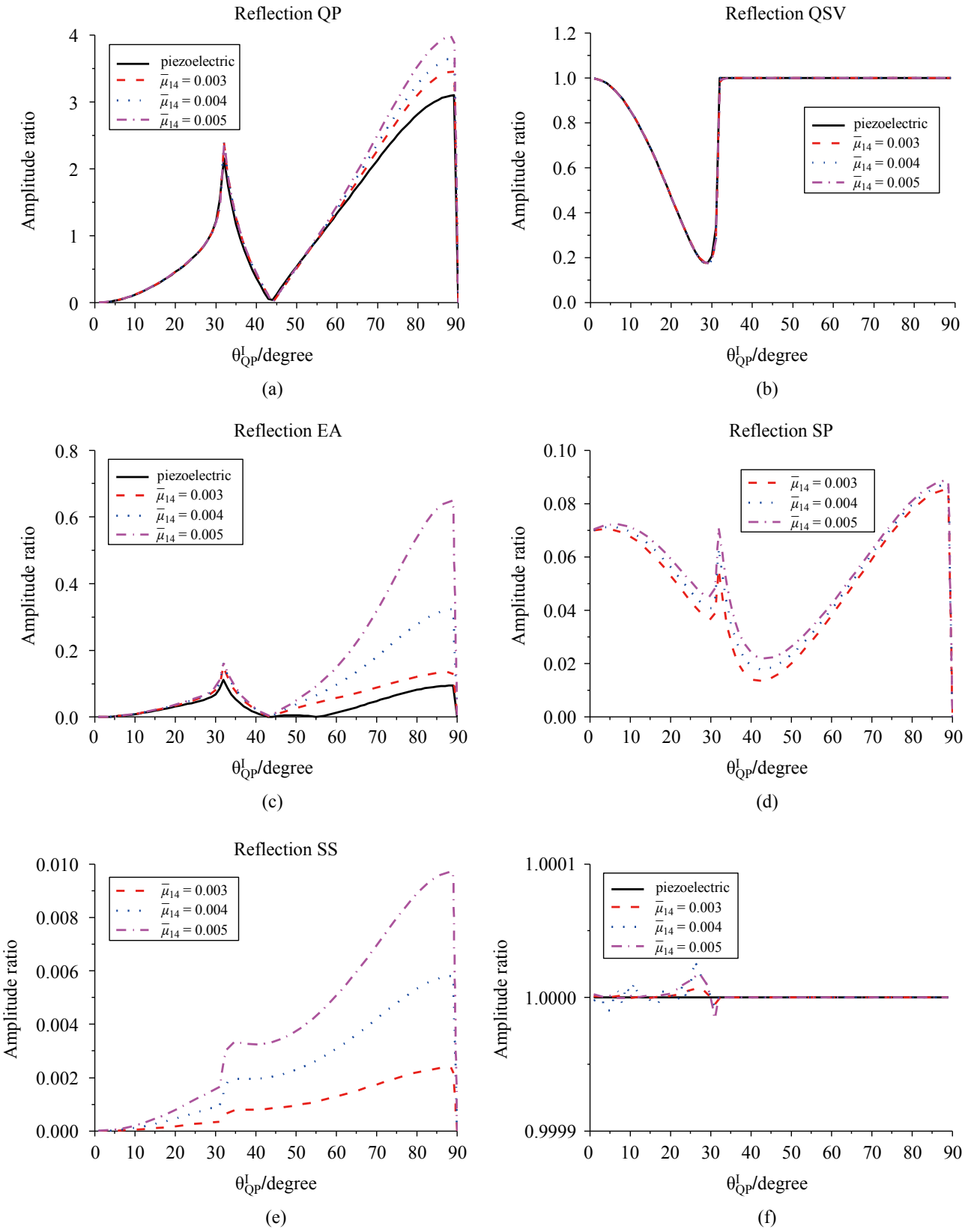


Fig. 4 The influences of flexoelectric coefficients on the amplitude ratios in the case of incident QSV wave and the check on the energy flux conservation. ($\bar{\mu}_{11}=0.5\bar{\mu}_{14}$, $\bar{\mu}_{111}=2\bar{\mu}_{14}$, $\bar{l}_1$=0.03, $\bar{l}_2=0.03$)

https://doi.org/10.1017/jmech.2017.87 Published online by Cambridge University Press

checked, see Fig. 3(f) and Fig. 4(f). It is noted that the energy conservation index E keeps near unit at the total range of incident angle with the large error smaller than one percent.

4. CONCLUSIONS

Any material is heterogeneous and has special microstructure at a sufficiently small scale. The homogeneous medium is only an approximation for actual medium at an enough large scale. In the wave problem, the medium is assumed homogeneous when the wave length of incident wave is enough large relative to the characteristic length of microstructure. When the wave length of incident wave is close to the characteristic length of microstructure, no matter whether the bulk material is at micro or nano scale, the microstructure effects cannot be ignored anymore. The approaches to deal with the microstructure effects are usually classified as two categories. The one regards the medium as heterogeneous and leads to the multiple scattering analysis; The other one still regards the medium as homogeneous but introduces some microstructure parameters to reflect the microstructure effects. The generalized elastic theory belongs to the latter. The present work is based on the generalized elastic theory and therefore belongs to the latter. The present work concerns the influences of the flexoelectric effect, the strain gradient effect and the micro-inertial effect upon the wave propagation at the high frequency range. It is found that both of the flexoelectric effect and the strain gradient effect make the propagation velocity of the elastic wave increase and have similar influences on the dispersive feature of QP wave and QSV wave in the piezoelectric solid. However, the micro-inertial effect has completely different influences. The existence of micro-inertial is vital in order to exhibit a physically acceptable dispersive feature at the high frequency range. Moreover, the flexoelectric effect, the strain gradient effect and the micro-inertial effect have more evident influences upon the surface waves than bulk waves. The fact that the surface waves are more sensitive to the flexoelectric effect and the strain gradient effect can be expected to obtain more microstructure information from the various surface waves measured experimentally by an inverse approach.

ACKNOWLEDGEMENTS

The work is supported by Fundamental Research Funds for the Central Universities (FRF-BR-15-026A) and National Natural Science Foundation of China (No. 10972029).

APPENDIX A

$$\mathbf{G}_{11}=\begin{bmatrix} c_{11} & 0 & 0 & c_{12} & 0 & 0 \\ 0 & c_{11} & 0 & 0 & c_{12} & 0 \\ 0 & 0 & c_{11} & 0 & 0 & c_{12} \\ c_{12} & 0 & 0 & c_{11} & 0 & 0 \\ 0 & c_{12} & 0 & 0 & c_{11} & 0 \\ 0 & 0 & c_{12} & 0 & 0 & c_{11} \end{bmatrix},\quad \mathbf{G}_{12}=\mathbf{G}_{21}^{\mathrm{T}}=\begin{bmatrix} c_{13} & 0 & 0 & 0 & 0 & 0 \\ 0 & c_{13} & 0 & 0 & 0 & 0 \\ 0 & 0 & c_{13} & 0 & 0 & 0 \\ c_{13} & 0 & 0 & 0 & 0 & 0 \\ 0 & c_{13} & 0 & 0 & 0 & 0 \\ 0 & 0 & c_{13} & 0 & 0 & 0 \end{bmatrix},$$

$$\mathbf{G}_{22}=\begin{bmatrix} c_{33} & 0 & 0 & 0 & 0 & 0 \\ 0 & c_{33} & 0 & 0 & 0 & 0 \\ 0 & 0 & c_{33} & 0 & 0 & 0 \\ 0 & 0 & 0 & c_{44} & 0 & 0 \\ 0 & 0 & 0 & 0 & c_{44} & 0 \\ 0 & 0 & 0 & 0 & 0 & c_{44} \end{bmatrix},\quad \mathbf{G}_{33}=\begin{bmatrix} c_{44} & 0 & 0 & 0 & 0 & 0 \\ 0 & c_{44} & 0 & 0 & 0 & 0 \\ 0 & 0 & c_{44} & 0 & 0 & 0 \\ 0 & 0 & 0 & 0.5(c_{11}-c_{12}) & 0 & 0 \\ 0 & 0 & 0 & 0 & 0.5(c_{11}-c_{12}) & 0 \\ 0 & 0 & 0 & 0 & 0 & 0.5(c_{11}-c_{12}) \end{bmatrix},$$

$$\mathbf{G}_{13}=\mathbf{G}_{23}=\mathbf{G}_{31}=\mathbf{G}_{32}=[\mathbf{0}]_{6\times 6}.$$

https://doi.org/10.1017/jmech.2017.87 Published online by Cambridge University Press

APPENDIX B

$$K_{11}=c_{11}+c_{44}\alpha^2+l_1^2\xi^2\left[c_{11}+\left(c_{11}+c_{44}\right)\alpha^2+c_{44}\alpha^4\right]-\rho c^2-\rho l_2^2\xi^2c^2\left(1+\alpha^2\right)/3,$$

$$K_{12}=K_{21}=\left(c_{13}+c_{44}\right)\alpha+\left(c_{13}+c_{44}\right)l_1^2\xi^2\alpha\left(1+\alpha^2\right),\quad K_{13}=\left(e_{15}+e_{31}\right)\alpha-i\mu_{11}\xi-i\left(\mu_{14}+2\mu_{111}\right)\xi\alpha^2,$$

$$K_{22}=c_{44}+c_{33}\alpha^2+l_1^2\xi^2\left[c_{44}+\left(c_{33}+c_{44}\right)\alpha^2+c_{33}\alpha^4\right]-\rho c^2-\rho l_2^2\xi^2c^2\left(1+\alpha^2\right)/3,$$

$$K_{23}=e_{15}+e_{33}\alpha^2-i\mu_{11}\xi\alpha^3-i\left(\mu_{14}+2\mu_{111}\right)\xi\alpha,\quad K_{33}=-\varepsilon_{11}-\varepsilon_{33}\alpha^2,$$

$$K_{31}=\left(e_{15}+e_{31}\right)\alpha+i\mu_{11}\xi+i\left(\mu_{14}+2\mu_{111}\right)\xi\alpha^2,\quad K_{32}=e_{15}+e_{33}\alpha^2+i\mu_{11}\xi\alpha^3+i\left(\mu_{14}+2\mu_{111}\right)\xi\alpha.$$

APPENDIX C

$$F_{1q}=c_{44}\left(\alpha_q+G_q\right)+e_{15}H_q,\quad F_{2q}=c_{13}+c_{33}\alpha_qG_q+e_{33}\alpha_qH_q,\quad F_{3q}=c_{11}+c_{13}\alpha_qG_q+e_{31}\alpha_qH_q,$$

$$F_{4q}=e_{31}+e_{33}\alpha_qG_q-\varepsilon_{33}\alpha_qH_q+i\xi\left[\mu_{11}G_q\alpha_q^2+\mu_{14}\alpha_q+\mu_{111}\left(\alpha_q+G_q\right)\right],$$

$$F_{5q}=e_{15}\left(\alpha_q+G_q\right)-\varepsilon_{11}H_q+i\xi\left[\mu_{11}+\mu_{14}G_q\alpha_q+\mu_{111}\left(\alpha_q+G_q\right)\alpha_q\right],$$

$$F_{6q}=i\xi\mu_{111}H_q\alpha_q-l_1^2\xi^2c_{44}\left(G_q+\alpha_q\right),\quad F_{7q}=i\xi\mu_{111}H_q-l_1^2\xi^2c_{44}\left(G_q+\alpha_q\right)\alpha_q,$$

$$F_{8q}=i\xi\mu_{14}H_q-l_1^2\xi^2\left(c_{13}+c_{33}G_q\alpha_q\right),\quad F_{9q}=i\xi\mu_{11}H_q\alpha_q-l_1^2\xi^2\left(c_{13}+c_{33}G_q\alpha_q\right)\alpha_q,$$

$$F_{10q}=i\xi\mu_{11}H_q-l_1^2\xi^2\left(c_{11}+c_{13}G_q\alpha_q\right),\quad F_{11q}=i\xi\mu_{14}H_q\alpha_q-l_1^2\xi^2\left(c_{11}+c_{13}G_q\alpha_q\right)\alpha_q.$$

REFERENCES

1. Alshits, V. I., Darinskii, A. N. and Shuvalov, A. L., "Theory of Reflection of Acoustoelectric Waves in Semi-Infinite Piezoelectric Medium. I. Metallized Surface," *Kristallografiya*, **34**, pp. 1340-1348 (1989).
2. Alshits, V. I., Darinskii, A. N. and Shuvalov, A. L., "Theory of Reflection of Acoustoelectric Waves in a Semiinfinite Piezoelectric Medium. III: Resonance Reflection in the Neighborhood of a Branch of Outflowing Waves," *Soviet Physics Crystallography*, **36**, pp. 145-153 (1991).
3. Singh, B., "Wave Propagation in a Prestressed Piezoelectric Half-Space," *Acta Mechanica*, **211**, pp. 337-344 (2010).
4. Pang, Y., Wang, Y. S., Liu, J. X. and Fang, D. N., "Reflection and Refraction of Plane Waves at the Interface between Piezoelectric and Piezomagnetic Media," *International Journal of Engineering Science*, **46**, pp. 1098-1110 (2008).
5. Abd-Alla, A. E. N. N. and Alsheikh, F. A., "Reflection and Refraction of Plane Quasi-Longitudinal Waves at an Interface of Two Piezoelectric Media under Initial Stresses," *Archive of Applied Mechanics*, **79**, pp. 843-857 (2009).
6. Guo, X. and Wei, P., "Effects of Initial Stress on the Reflection and Transmission Waves at the Interface between Two Piezoelectric Half Spaces," *International Journal of Solids and Structures*, **51**, pp. 3735-3751 (2014).
7. Guo, X., Wei, P. and Li, L., "Dispersion Relations of Elastic Waves in One-Dimensional Piezoelectric Phononic Crystal with Mechanically and Dielectrically Imperfect Interfaces," *Mechanics of Materials*, **93**, pp. 168-183 (2016).
8. Zubko, P., Catalan, G. and Tagantsev, A. K., "Flexoelectric Effect in Solids," *Annual Review of Materials Research*, **43**, pp. 387-421 (2013).
9. Hu, S. and Shen, S., "Electric Field Gradient Theory with Surface Effect for Nano-Dielectrics," *Computers, Materials & Continua (CMC)*, **13**, pp. 63-88 (2009).
10. Hu, S. and Shen, S., "Variational Principles and Governing Equations in Nano-Dielectrics with the Flexoelectric Effect," *SCIENCE CHINA Physics, Mechanics & Astronomy*, **53**, pp. 1497-1504 (2010).
11. Shu, L., Wei, X., Pang, T., Yao, X. and Wang, C., "Symmetry of Flexoelectric Coefficients in Crystalline Medium," *Journal of Applied Physics*, **110**, 104106 (2011).
12. Qi, L., Zhou, S. and Li, A., "Size-Dependent Bending of an Electro-Elastic Bilayer Nanobeam Due to Flexoelectricity and Strain Gradient Elastic Effect,"

https://doi.org/10.1017/jmech.2017.87 Published online by Cambridge University Press

Composite Structures, **135**, pp. 167-175 (2016).

13. Liang, X., Hu, S. and Shen, S., "Bernoulli–Euler Dielectric Beam Model Based on Strain-Gradient Effect," *Journal of Applied Mechanics*, **80**, 044502 (2013).
14. Ebrahimi, F. and Barati, M. R., "Surface Effects on the Vibration Behavior of Flexoelectric Nanobeams Based on Nonlocal Elasticity Theory," *The European Physical Journal Plus*, **1**, pp. 1-13 (2017).
15. Liu, C. and Wang, J., "Size-Dependent Electromechanical Properties in Piezoelectric Superlattices Due to Flexoelectric Effect," *Theoretical and Applied Mechanics Letters*, **7**, pp. 88-92 (2017).
16. Xu, L. and Shen, S., "Size-Dependent Piezoelectricity and Elasticity Due to the Electric Field-Strain Gradient Coupling and Strain Gradient Elasticity," *International Journal of Applied Mechanics*, **5**, 1350015 (2013).
17. Li, Y. and Wei, P., "Reflection and Transmission of Plane Waves at the Interface between Two Different Dipolar Gradient Elastic Half-Spaces," *International Journal of Solids and Structures*, **56**, pp. 194-208 (2015).

(Manuscript received April 20, 2017,
accepted for publication July 31, 2017.)

https://doi.org/10.1017/jmech.2017.87 Published online by Cambridge University Press